Neurons sense nanoscale roughness with nanometer sensitivity

V. Brunetti, G. Maiorano, L. Rizzello, B. Sorce, S. Sabella, R. Cingolani, and P. P. Pompa[1]

Italian Institute of Technology, Center for Bio-Molecular Nanotechnology, Via Barsanti, 1-73010 Arnesano (Lecce), Italy

Edited by Michael P. Sheetz, Columbia University, New York, NY, and accepted by the Editorial Board February 23, 2010 (received for review December 15, 2009)

The interaction between cells and nanostructured materials is attracting increasing interest, because of the possibility to open up novel concepts for the design of smart nanobiomaterials with active biological functionalities. In this frame we investigated the response of human neuroblastoma cell line (SH-SY5Y) to gold surfaces with different levels of nanoroughness. To achieve a precise control of the nanoroughness with nanometer resolution, we exploited a wet chemistry approach based on spontaneous galvanic displacement reaction. We demonstrated that neurons sense and actively respond to the surface nanotopography, with a surprising sensitivity to variations of few nanometers. We showed that focal adhesion complexes, which allow cellular sensing, are strongly affected by nanostructured surfaces, leading to a marked decrease in cell adhesion. Moreover, cells adherent on nanorough surfaces exhibit loss of neuron polarity, Golgi apparatus fragmentation, nuclear condensation, and actin cytoskeleton that is not functionally organized. Apoptosis/necrosis assays established that nanoscale features induce cell death by necrosis, with a trend directly related to roughness values. Finally, by seeding SH-SY5Y cells onto micropatterned flat and nanorough gold surfaces, we demonstrated the possibility to realize substrates with cytophilic or cytophobic behavior, simply by fine-tuning their surface topography at nanometer scale. Specific and functional adhesion of cells occurred only onto flat gold stripes, with a clear self-alignment of neurons, delivering a simple and elegant approach for the design and development of biomaterials with precise nanostructure-triggered biological responses.

nanobiointeractions | nanostructures | patterning

The potential of nanomaterials to trigger specific cellular responses, such as interference and/or activation of defined pathways (1–3), is promising for the development of many important scientific fields, such as regenerative medicine, biotechnology, drug delivery, and nanotoxicity assessment. Initially, cells–materials interactions were tackled only from a chemical point of view, because environmental sensing by cells involves specific binding between cellular receptors and ECM ligands. However, recently there has been increasing evidence that the biological response is also affected by the physical properties of the material (4). In particular, it has been demonstrated that cells are influenced by the substrate topography (5, 6), rigidity (7, 8), anisotropy (9, 10), surface charge (11, 12), and wettability (13, 14). From this perspective, cellular response to external stimuli goes far beyond the bare ability of the cell to chemically sense specific ECM ligands and includes a wide range of physical cues that are generated at, or act on, the interface between cells and the surrounding environment. For instance, it has been observed that micrometer-scale roughness may affect cell proliferation and morphology (15, 16), because it provides a quasi-biomimetic microenvironment to the cells. However, cell–substrate interactions are typically governed by complex mechanisms occurring at the nanoscale, which are generally referred to as nanobiointeractions (17). In fact, because the adhesion sites of the cell (focal adhesions) are in the range of 5–200 nm, it is clear that these very small cellular components may be strongly influenced by nanoscale features rather than microscale structures (18). In this frame, nanofabrication techniques may offer interesting tools to achieve a precise control of the surface properties (e.g., controlled nanotexture) and, thus, to evaluate the mechanisms and spatiotemporal aspects of nanomaterial interactions with living systems (19–23). In this work, we investigated the biological response of human neuroblastoma cells (SH-SY5Y) upon interaction with highly controlled nanostructured metal substrates. Neural cells are known to be strongly affected by the properties of culture substrates (24). In particular, the SH-SY5Y cell line is a good model for neuronal differentiation and shows an integrin receptors pathway highly sensitive to environmental stimuli (25, 26). To evaluate the effects that surface nanoroughness may exert over these neuronal cells, we applied a wet chemistry technique, namely, spontaneous galvanic displacement reactions (SGDR) (27) that can allow an extremely precise control over the surface morphology. SGDR enabled us to reliably fabricate surface nanoscale features with accurate and controlled levels of surface nanoroughness, uniformly extended over wide areas. We demonstrated that nanostructured gold surfaces can modulate neurons behavior with a direct dependence on surface nanoroughness. Interestingly, such nanotopographies are able to trigger neuron adhesion/viability, with a surprising sensitivity of cells to nanometer-scale changes. Moreover, by combining SGDR processes with lithographic techniques (27, 28), we demonstrated the possibility to obtain two-dimensional micropatterns of cytophilic/cytophobic surfaces, respectively presenting permissive or hostile signals for cell adhesion. This approach leads to a clear self-alignment of neuronal cells, simply by tuning the surface nanoscale features.

Results and Discussion

In what follows, we discuss how surface nanoroughness influences the biological response of neurons, namely, cell adhesion, morphology, differentiation, and, ultimately, cell survival. We studied SH-SY5Y cells as a model system for their particular sensitivity to environmental stimuli (25, 26) and for the importance of functional biomaterials in neural research. To obtain a good control of surface topography, we exploited a wet chemistry approach (SGDR) (27), achieving different nanorough gold surfaces (Fig. 1). By tuning the thickness of the initial sacrificial metal, we were able to obtain increasing values of surface roughness with nanometer control and appreciable uniformity. Fig. 1 depicts the atomic force microscopy (AFM) analyses of the nanostructured surfaces employed for the cell growth. It is interesting to note the precise control of the surface nanoroughness, with the mean rough values (R_a) increasing from *ca.* 36 nm of the first nanostructured sample (Fig. 1*B*) to an R_a value of 100 nm of the most rough substrate (Fig. 1*F*). On the other hand, the reference flat Au surface exhibits an R_a value less than 1 nm (Fig. 1*A*). AFM

Author contributions: V.B. and P.P.P. designed research; V.B., G.M., L.R., B.S., and P.P.P. performed research; V.B., G.M., L.R., B.S., S.S., R.C., and P.P.P. analyzed data; and V.B., G.M., L.R., B.S., S.S., R.C., and P.P.P. wrote the paper.

The authors declare no conflict of interest.

This article is a PNAS Direct Submission. M.P.S. is a guest editor invited by the Editorial Board.

[1]To whom correspondence should be addressed. E-mail: piero.pompa@unile.it.

line profiles (Fig. 1 *B–E*, *Bottom*) of the rough substrates confirmed the precise control of the surface morphology, revealing a homogeneous increase of nanoroughness in the different samples. All these gold substrates were chemically modified with cysteine coating to provide a "biologically friendly" surface for cells. In the early moments of cell contact with substrates, proteins in the medium adsorb onto material surfaces (16), mediating the subsequent cellular events such as adhesion, proliferation, and differentiation (29). Cysteine-functionalized substrates exhibit a marked hydrophilic character, which raises with the increase of R_a (28). The first investigation was directed to estimate cell adhesion onto the different nanotopographies. Fig. 2*A* reveals a significant decrease of cell attachment on the nanostructured substrates, directly related to the nanoroughness level. Interestingly, small differences in R_a (even a few nanometers) are clearly sensed by the cells that exhibit different adhesion capability. At the highest value of R_a (80–100 nm), we observed a dramatic decrease of cell adhesion, down to about 10–15% of the control flat substrate. A further investigation aimed to explore cell fate after interaction and adhesion onto such nanotopographies. We performed a test capable to distinguish between apoptotic and necrotic cells, on the basis of in vivo staining with FITC-conjugated annexinV and propidium iodide (PI). Fig. 2*B* elucidates the dependence of cell fate as a function of nanoroughness. It is possible to note that substrate nanostructuration, besides hindering cell adhesion, strongly elicits necrosis processes in SH-SY5Y cells, with a trend directly related to the R_a value. Noteworthy, even in the substrate with the minimal R_a value (36 nm), *ca.* 50% of adherent cells undergo necrosis processes. Then, in the other more rough substrates, cell necrosis approaches 90–95%. On the other hand, no pathways of programmed cell death were induced by nanostructuration: Apoptotic cell percentage remains constant among the different nanorough substrates and similar to the value found on the control surface. The investigated R_a values are comparable with the dimension of protein complexes, so SH-SY5Y were influenced by the different nanobiointeractions that are generated at the interface between cell and nanostructuration. To investigate this cellular behavior, we performed confocal imaging of SH-SY5Y cells cultured for 24 h onto flat (Fig. 3*A*) and nanorough substrates (Fig. 3*B*, substrate with R_a value of 100 nm). As expected, flat gold surface allows specific cell adhesion, axonal autogrowth, and functional cytoskeletal orientation, whereas nuclei maintain their integrity, showing finely dispersed chromatin. On the other side, the few cells grown onto nanorough substrates showed a round shape, a tendency to form clusters, and a lack of specialized structures. The nucleus results condensed, and the filamentous actin structures were localized in the peripheral area of cytoplasm, suggesting that these cells are undergoing necrosis, in line with the findings of Fig. 2*B*.

To further understand the cell–nanostructure interactions, we investigated the cellular sensing machinery, namely, the focal adhesion points. Because such a dynamic complex mediates the adhesion-dependent recruitment of signaling molecules, which are essential for cell response to environmental stimuli (4, 30), we decided to explore the distribution and recruitment of vinculin, an ubiquitously expressed cytoskeletal protein (31). SH-SY5Y cells cultured onto flat surfaces (Fig. 4 *A–B*) presented a clear pattern of adhesion complexes, identified as green spots (vinculin aggregates) that are mainly localized at the periphery of the cell, in connection with axonal growth. Such a protein is indeed associated in characteristic plaques during formation of focal adhesion complex (31–33). Cells seeded onto rough substrates (Fig. 4 *C–D*), conversely, showed a sporadic and not organized distribution of vinculin plaques. These results clearly support the concept that surface nanotopography affects cell

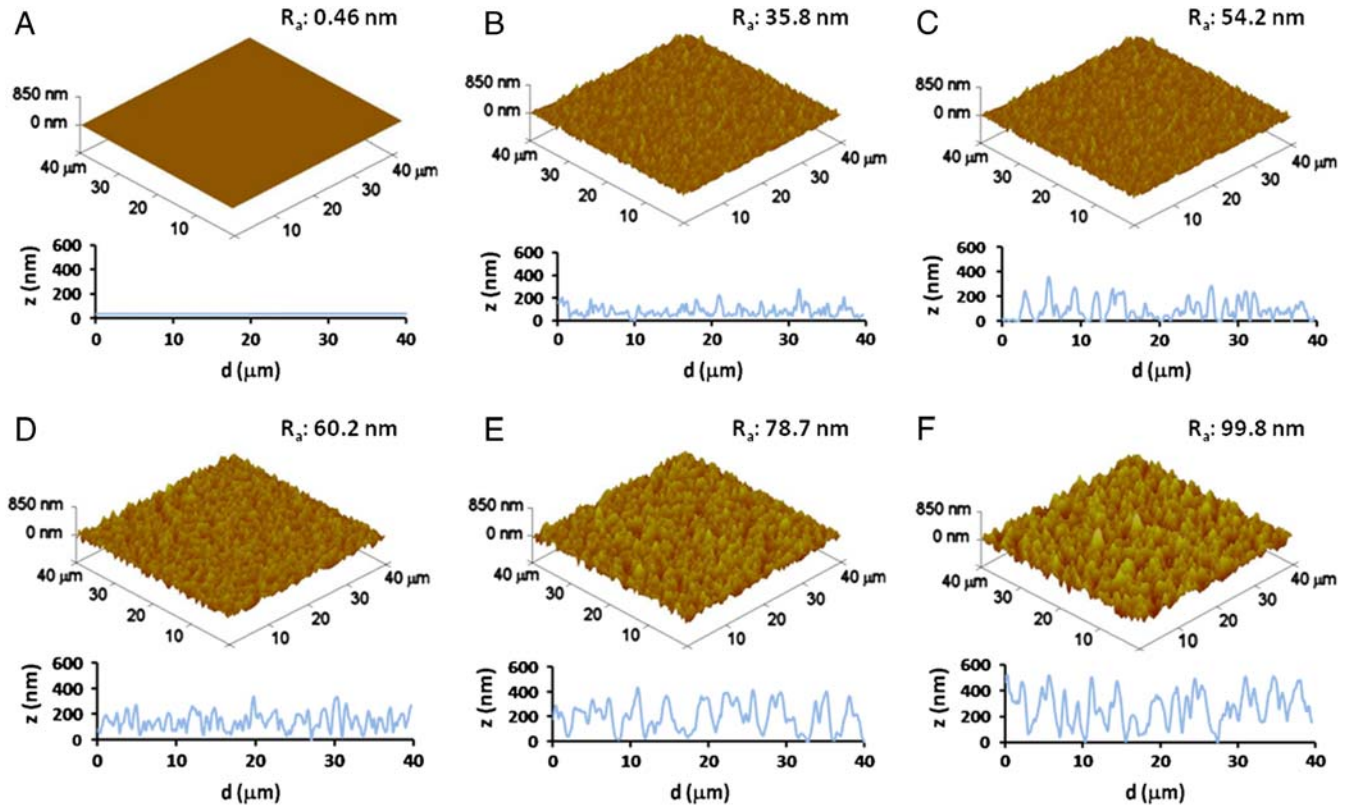

Fig. 1. AFM analysis of gold surfaces with increasing level of nanoroughness. The surface morphology shifts from a flat gold film (*A*) to uniformly nanostructured surface with different level of nanoroughness (*B–E*). R_a indicates the mean surface roughness, calculated on 40×40 μm^2 regions. On the bottom of each substrate, representative line profiles are reported.

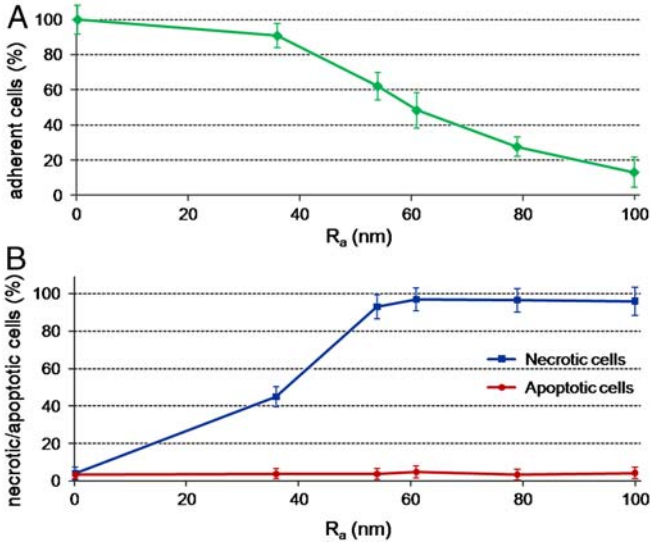

Fig. 2. (*A*) SH-SY5Y cell adhesion onto different nanostructured gold surfaces with increasing values of nanoroughness (from 0 to 100 nm R_a), after 24 h of culture. (*B*) AnnexinV-FITC/PI in vivo staining of SH-SY5Y cells cultured for 24 h onto substrates with different nanoroughness. By this test, it was possible to distinguish and count between apoptotic cells (AnnexinV$^+$/PI$^-$), necrotic cells (AnnexinV$^-$/PI$^+$), and viable cells (AnnexinV$^-$/PI$^-$).

behavior via a direct mechanism. A possible contribution may be provided by the increasing hydrophilicity of the rough substrates (28), which may affect the correct formation of the ECM layer onto the substrate. The observed cell response may be explained by the properties of nanorough surfaces to influence the adsorption of cell adhesive serum proteins, such as fibronectin and laminin, in terms of composition and/or correct folding of the adsorbed protein layers. This class of proteins plays a critical role in neurons adhesion and growth (34, 35). An inappropriate protein coating formation onto nanorough surfaces may lead to inadequate clustering of the right amount of integrins and thus to a poor and disorganized recruitment of vinculin, necessary for stable and mature focal adhesion complexes (36). In this respect, we observed that the sensing cellular machinery of SH-SY5Y cells is not able to correctly interact with the nanorough substrates. As a result, the absence of functional focal adhesion points deprives neurons of survival integrin-mediated signaling and intracellular signaling of anchorage-dependent growth (29, 37). This evidence is in qualitative agreement with the necrosis processes observed in Figs. 2*B* and 3*B*.

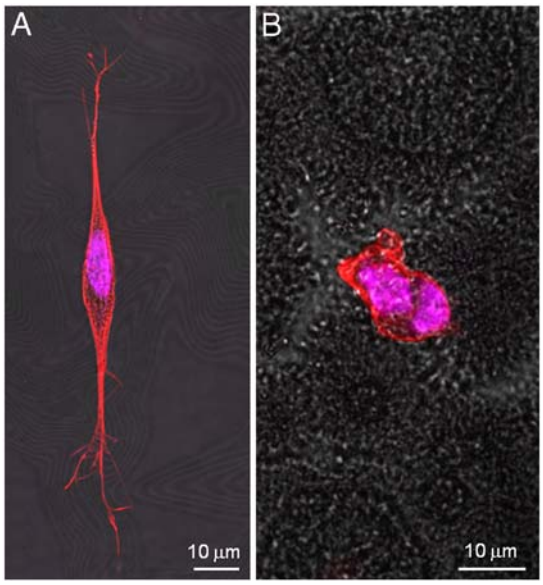

Fig. 3. Confocal images of SH-SY5Y cultured onto (*A*) flat and (*B*) nanorough (R_a = 100 nm) surfaces. Cells were incubated with Phalloidin-TRITC conjugate for actin cytoskeleton staining and with Hoechst 33258 for nuclei staining.

Another important point is the assessment of neuron functionality in terms of their Golgi apparatus morphology. In fact, Golgi belongs to the organelles of the neuronal secretory pathway, with a crucial role for neuronal development as well as for the proper localization of plasma membrane proteins necessary for polarity, synaptic transmission, and plasticity (38). Fig. 5 reports immunodetection of Golgi complex by anti-golgin 97 antibody that recognizes the 97 kDa protein golgin-97, a peripheral membrane protein localized on the cytoplasmic face of the Golgi apparatus, that plays a critical role in vesicle traffic from the endosome to the trans-Golgi network (39). SH-SY5Y cells cultured onto the flat surface (Fig. 5 *A–B*) exhibit a well-developed Golgi system, indicating a good cellular functionality. In particular, a wide network of distal Golgi vesicles for the entire length of axons is evident. Such structures are important during the phase of neuron growth, being involved in the trafficking of both integral membrane proteins and the secreted neuronal growth factors (38). Such a well-distributed Golgi complex reinforces the evidence of fully developed and functional SH-SY5Y cells. On the other hand, cells seeded onto a nanorough surface (Fig. 5 *C–D*) have the typical Golgi features of cells undergoing the necrosis process (40), likely because of the extensive cytoplasmic damage associated to necrosis. In particular, Fig. 5 *C–D* depicts an inactive Golgi network, leaned against the nuclear membrane, with no evidence of polarity. These results show that cells cultured onto flat surfaces present a polarized organization of neuronal secretory trafficking and demonstrate a possible link between membrane trafficking and cellular nanotopography sensing.

Finally, we demonstrated the possibility to control cell adhesion and proliferation onto micropatterned substrates with alternated flat and nanorough surfaces, showing that the control of such nanotopographies can guide substrates toward cytophilic or cytophobic behavior. In this respect, neurons cultured onto 100 μm (Fig. 6 *A–C*) or 50 μm (Fig. 6*D*) of flat/nanorough patterned stripes show, in fact, selective growth onto the flat stripes, in close agreement with the results presented above. Therefore, by only varying the surface nanostructuration, neuronal cell adhesion and growth can be easily and precisely controlled. In particular, cells actively choosing flat surfaces present specific cell adhesion, axonal autogrowth, axonal pathfinding, and cytoskeletal specific orientation, as elucidated by Fig. 6, in which nuclei and actin cytoskeleton network are stained. This result shows that nanoscale features, alone, are able to control and guide SH-SY5Y cell adhesion, proliferation, and fate, opening an interesting perspective for efficient and functional neuron patterning.

Conclusions

Our results demonstrated that SH-SY5Y neuronal cells have a surprisingly high sensitivity to nanoscale features. The surface nanoroughness represents the main driving force that actively influences adhesion, development, and functionality of SH-SY5Y cells. Adherent cells, focal adhesion points, cytoskeleton, Golgi organization, and morphology were investigated, revealing a striking difference between cells adhering onto nanorough surfaces with respect to flat samples. The lack of organized focal adhesion points triggers a cascade of signaling processes that produces loss of neuron polarization and activity, by disruption of a coordinated regulation of membrane trafficking and of cytoskeletal dynamics, leading to necrosis. It is remarkable that also small values of surface nanoroughness are able to generate a massive biological response in terms of cell viability. An

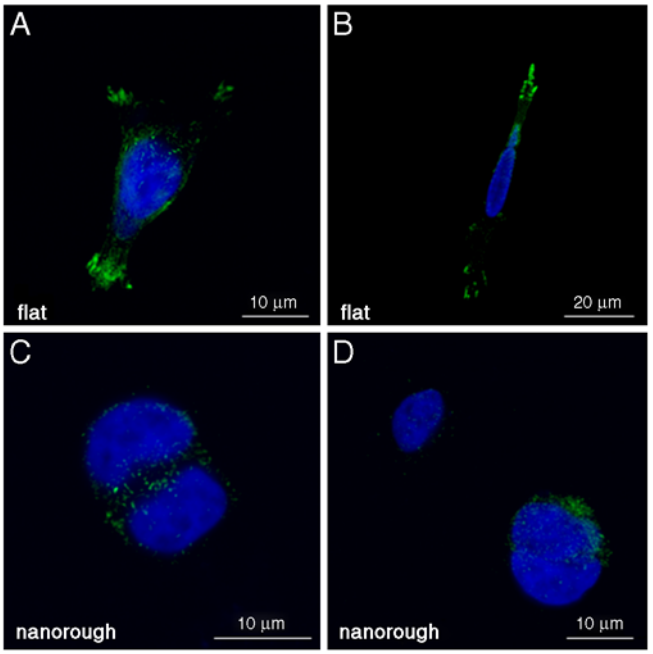

Fig. 4. Confocal images of SH-SY5Y cultured onto flat (*A*, *B*) and nanorough (*C*, *D*) surfaces. Cells were stained with antivinculin antibodies to mark focal adhesions (*Green*) and Hoechst 33258 (*Blue*) for nuclei labeling.

important consequence of nanoscale engineering of biomaterials surface is that nanotopography alone can be used to guide different biological responses, starting from the same cell. In fact, in the micropatterned flat/nanorough gold surfaces, we observed cell adhesion and cytoskeletal specific orientation only in the smooth gold areas of the substrates, resulting in a clear self-alignment of neuronal cells. These results were achieved simply by varying nanoscale features, combining lithographic techniques with a wet chemistry approach (SGDR), without any complex strategy of biomolecule selective patterning. In conclusion, by properly controlling and managing the surface features, we were able to realize cytophilic or cytophobic surfaces, useful in the development of biomaterials for neural research, ranging from basic biological studies to tissue engineering.

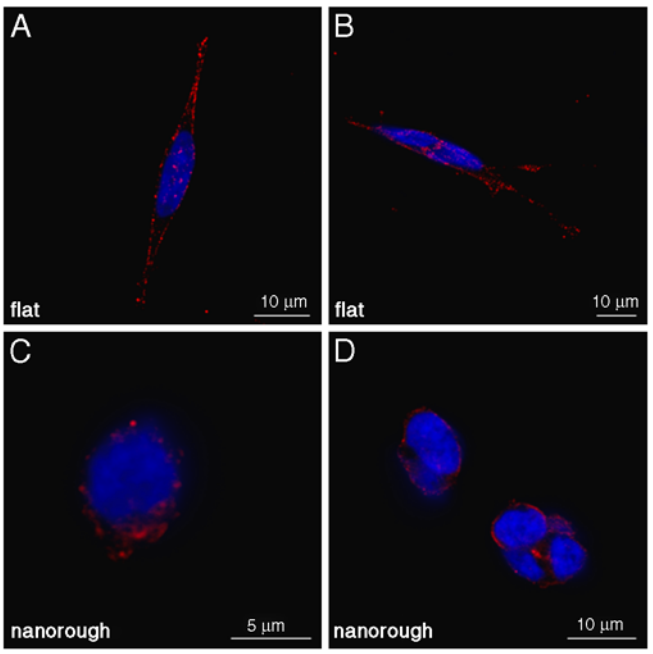

Fig. 5. Representative confocal images of SH-SY5Y cultured onto flat (*A*, *B*) and nanorough (*C*, *D*) surfaces. Cells were labeled with anti-golgin 97 antibodies to stain Golgi network (*Red*) and Hoechst 33258 (*Blue*) for nuclei staining.

Materials and Methods

Roughness-Controlled Gold Surfaces and Pattern Fabrication. To evaluate the effects of nanoscale features over cell behavior, we fabricated different substrates with increasing values of nanoroughness. For the preparation of substrates, glass slides (1.5 cm × 1.5 cm) were first sonicated with ultrapure water for 10 min and then treated with a 1:1:5 solution of 30% NH_3OH (J. T. Baker), 30% H_2O_2 (J. T. Baker), and water at 75 °C for 10 min, followed by treatment with a 1:1:5 solution of 30% HCl (J. T. Baker), 30% H_2O_2, and water at 75 °C for 10 min, with intermediate washing steps with deionized water after each treatment. Subsequently, the cleaned surfaces were reacted with 400 μL of 1% aminopropyltriethoxysilane (APTES, Sigma-Aldrich) aqueous solution for 5 min, washed with deionized water, and kept in vacuum overnight to remove the unbound APTES molecules. Such samples were coated with different thicknesses of Ag film, namely, 10, 20, 30, 40, and 50 nm, respectively, onto a predeposited 50-nm-thick flat Au film (0.5 Å/s evaporation rate). All these samples were then incubated, for the SGDR reaction, with the same $HAuCl_4$ (Sigma-Aldrich) aqueous solutions (10^{-3} M $HAuCl_4$, 10 min of incubation at room temperature), followed by extensive washing in deionized water and 5% vol/vol NH_3OH (J. T. Baker) for 10 min to remove the AgCl produced by the reaction and possibly adsorbed over the surface. In this way, by tuning the thickness of the initial sacrificial template for the SGDR process, we were able to conveniently tune the surface roughness, with nanometer control. A 50-nm-thick flat Au film was used as the reference substrate for cells. To further evaluate cellular response to nanostructured surface topologies, we fabricated patterned flat/nanorough gold samples (27). Cleaned APTES-modified substrates were first coated with a 50-nm-thick flat Au film (0.5 Å/s evaporation rate) and then 100- or 50-μm stripes mask of optical AZ® 9260 resist layers (Nowell) were defined on them, allowing the selective deposition of 50-nm-thick Ag film only within the exposed regions of the gold film. After removing the resist with acetone, the patterned Au-Ag substrates were incubated for 10 min with 10^{-3} M $HAuCl_4$ aqueous solution for the SGDR reaction, so only the Ag stripes were replaced by gold ions. To allow optimal cell adhesion onto flat and nanorough substrates, all samples were subsequently functionalized with cysteine (Sigma-Aldrich) solution (10^{-3} M overnight under nitrogen atmosphere). Such thiol/Au chemistry allowed us to uniformly cover both flat and rough gold surfaces with a monolayer of such a small molecule (28) that creates a biologically friendly surface. The topography of the gold surfaces was characterized by AFM. All AFM experiments were performed in contact mode in air, using a Nanoscope IV MultiMode scanning probe microscopy (Veeco Instruments) under ambient conditions (20–25 °C, atmospheric pressure, ~50% humidity). Ultrasharp silicon nitride AFM probes (DNP-S series; Veeco Instruments) were used with a typical spring constant of 0.58 N m^{-1} and a normal tip radius of 10 nm. Several images were obtained from separate locations of the surfaces to ensure reproducibility. All the images were analyzed by using the NanoScope™ software (Digital Instruments, version 6.0).

Cell Culture. Flat and nanostructured gold surfaces were sterilized by immersion in absolute ethanol (J. T. Baker) for 15 min and then dried in sterile hood. The SH-SY5Y human neuroblastoma cell line was routinely seeded at densities of 1×10^5 cells/cm^2 in high glucose (4, 500 mg/L) DMEM with 50 μM glutamine (Gibco), 1 mM sodium pyruvate (Gibco), and 0.1 mM nonessential amino acids (Gibco), supplemented with 10% FBS, 100 U/mL penicillin, and 100 mg/mL streptomycin (Invitrogen). Cells were incubated in a humidified controlled atmosphere with a 95% to 5% ratio of air/CO_2, at 37 °C. Medium was changed every 3 days. Subconfluent cultures were split once per week, by using 1× trypsin/EDTA (Invitrogen).

Confocal Microscopy for Adherent Cell Counting and for Apoptosis/Necrosis Assay. Counting of adherent SH-SY5Y cells onto flat and nanostructured substrates with an increasing level of nanoroughness was carried out by nuclei staining with Hoechst 33258 (Fluka). Briefly, each substrate was seeded with 1×10^5 cells/cm^2. After 24 h of incubation, samples were washed with PBS pH 7.4 (Sigma) to remove floating cells. Adherent cells were fixed in buffered 3.7% formaldehyde (Sigma) for 20 min, permeabilized with 0.1% Triton X-100 (Sigma) in PBS for 5 min, and subsequently incubated with 1 ng/mL Hoechst in PBS for nuclei fluorescent characterization and counting. An annexinV-FITC apoptosis kit (Sigma) was used for a direct count of viable, apoptotic, and necrotic cells onto flat and nanorough substrates. After

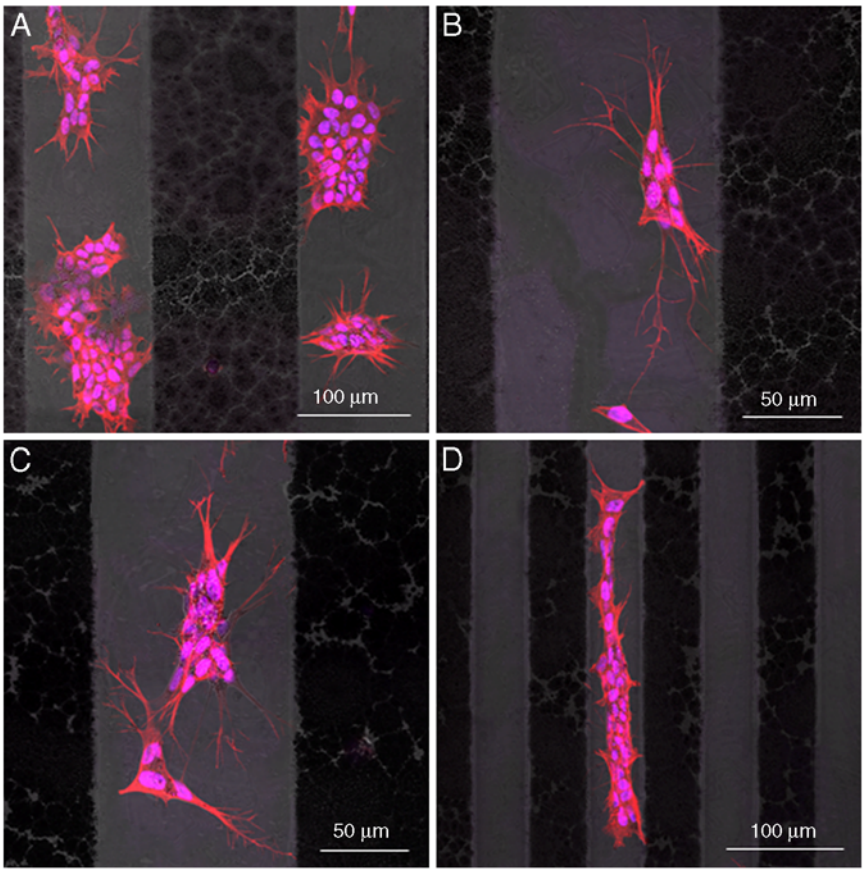

Fig. 6. Representative confocal images showing the selective adhesion of SH-SY5Y cultured onto flat/nanorough micropatterned 100-μm stripes (*A*–*C*) and 50-μm stripes (*D*). Cells were stained with Phalloidin-TRITC conjugate and with Hoechst 33258 for cytoskeleton and nuclei imaging, respectively.

24 h of incubation, samples were washed in binding buffer, incubated in the dark with annexinV-FITC and PI, as described in the manufacturer instructions. For both adherent and apoptotic/necrotic cell counting, we acquired 10 random fields for each sample by a confocal microscope (Leica TCS-SP5 AOBS). Samples were observed through a 20×, 0.70 N.A. objective. For statistical analysis and reproducibility verification, each experiment was performed with four biological replicates.

Confocal Microscopy for Cell Characterizations. SH-SY5Y cells, grown in the same conditions reported above, were fixed in formaldehyde, then permeabilized in Triton X-100, and blocked in PBS, 1% BSA, and 0.01% sodium azide for 15 min. Primary antibodies incubation was carried out for 1 h at room temperature at a dilution of 1:500 in blocking agent; secondary antibodies incubation was performed at the same conditions, at a dilution 1:1, 000 in blocking reagent. To detect focal adhesion points, Monoclonal Anti-Vinculin (Sigma-Aldrich) and Donkey Anti-Mouse IgG DyLight 488 (Jackson ImmunoResearch) were used. To characterize morphology and polarity of the Golgi apparatus, anti-golgin 97 (Molecular Probes) and Donkey Anti-Mouse DyLight 649 (Jackson ImmunoResearch) were used. In both preparations, nuclei were stained with Hoechst 33258 (Fluka). For cells cultured onto micropatterned flat/nanorough gold surfaces, cytoskeleton morphology was investigated by phalloidin-TRITC (Sigma) labeling (1 μg/mL in PBS from 1 mg/mL DMSO stock solution) and nuclei by Hoechst 33258 staining. After washing, all samples were mounted with Fluoromount (Sigma) on a glass coverslip and characterized by confocal microscopy. Samples were observed through a 20×, 0.70 N.A. objective or a 63×, 1.40 N.A. oil immersion objective.

ACKNOWLEDGMENTS. The authors gratefully acknowledge S. Shiv Shankar and G. Vecchio for useful discussions and V. Fiorelli for the expert technical assistance.

1. Mitragotri S, Lahann J (2009) Physical approaches to biomaterial design. *Nat Mater* 8:15–23.
2. Oh S, et al. (2009) Stem cell fate dictated solely by altered nanotube dimension. *Proc Natl Acad Sci USA* 106:2130–2135.
3. Chen CS, Mrksich M, Huang S, Whitesides GM, Ingber DE (1997) Geometric control of cell life and death. *Science* 276:1425–1428.
4. Geiger B, Spatz JP, Bershadsky AD (2009) Environmental sensing through focal adhesions. *Nat Rev Mol Cell Biol* 10:21–33.
5. Spatz JP, Geiger B (2007) Molecular engineering of cellular environments: Cell adhesion to nano-digital surfaces. *Methods Cell Biol* 83:89–111.
6. Vogel V, Sheetz M (2006) Local force and geometry sensing regulate cell functions. *Nat Rev Mol Cell Biol* 7:265–275.
7. Engler AJ, Sen S, Sweeney HL, Discher DE (2006) Matrix elasticity directs stem cell lineage specification. *Cell* 126:677–689.
8. Discher DE, Janmey P, Wang YL (2005) Tissue cells feel and respond to the stiffness of their substrate. *Science* 310:1139–1143.
9. Théry M, et al. (2006) Anisotropy of cell adhesive microenvironment governs cell internal organization and orientation of polarity. *Proc Natl Acad Sci USA* 103:19771–19776.
10. Xia N, et al. (2008) Directional control of cell motility through focal adhesion positioning and spatial control of Rac activation. *FASEB J* 22:1649–1659.
11. Ohgaki M, Kizuki T, Katsura M, Yamashita K (2001) Manipulation of selective cell adhesion and growth by surface charges of electrically polarized hydroxyapatite. *J Biomed Mater Res* 57:366–373.
12. Xu Y, Takai M, Ishihara K (2009) Protein adsorption and cell adhesion on cationic, neutral, and anionic 2-methacryloyloxyethyl phosphorylcholine copolymer surfaces. *Biomaterials* 30:4930–4938.
13. Velzenberger E, El Kirat K, Legeay G, Nagel MD, Pezron I (2009) Characterization of biomaterials polar interactions in physiological conditions using liquid-liquid contact angle measurements: Relation to fibronectin adsorption. *Colloids Surface B* 68:238–244.
14. Wei J, et al. (2009) Influence of surface wettability on competitive protein adsorption and initial attachment of osteoblasts. *Biomed Mater* 4:045002.
15. Karuri NW, et al. (2004) Biological length scale topography enhances cell-substratum adhesion of human corneal epithelial cells. *J Cell Sci* 117:3153–3164.
16. Brunette DM, Chehroudi B (1999) The effects of the surface topography of micromachined titanium substrata on cell behavior *in vitro* and *in vivo*. *J Biomech Eng* 121:49–57.

17. Curtis AS, Dalby M, Gadegaard N (2006) Cell signaling arising from nanotopography: implications for nanomedical devices. *Nanomedicine* 1:67–72.
18. Arnold M, et al. (2004) Activation of integrin function by nanopatterned adhesive interface. *ChemPhysChem* 5:383–588.
19. Vetrone F, et al. (2009) Nanoscale oxidative patterning of metallic surfaces to modulate cell activity and fate. *Nano Lett* 9:659–665.
20. Choi CH, et al. (2007) Cell interaction with three-dimensional sharp-tip nanotopography. *Biomaterials* 28:1672–1679.
21. Akiyama H, Ito A, Kawabe Y, Kamihira M (2010) Cell-patterning using poly (ethylene glycol)-modified magnetite nanoparticles. *J Biomed Mater Res A* 3:1123–1130.
22. Fredin NJ, Broderick AH, Buck ME, Lynn DM (2009) Nanoimprinted thin films of reactive, azlactone-containing polymers: Combining methods for the topographic patterning of cell substrates with opportunities for facile post-fabrication chemical functionalization. *Biomacromolecules* 10:994–1003.
23. Cavalcanti-Adam EA, et al. (2007) Cell spreading and focal adhesion dynamics are regulated by spacing of integrin ligands. *Biophys J* 92:2964–2974.
24. Millaruelo AI, Nieto-Sampedro M, Cotman CW (1988) Cooperation between nerve growth factor and laminin or fibronectin in promoting sensory neuron survival and neurite outgrowth. *Brain Res* 466:219–228.
25. Caltagarone J, Jing Z, Bowser R (2007) Focal adhesions regulate Abeta signaling and cell death in Alzheimer's disease. *Biochim Biophys Acta* 1772:438–445.
26. Buttiglione M, et al. (2007) Behaviour of SH-SY5Y neuroblastoma cell line grown in different media and on different chemically modified substrates. *Biomaterials* 28:2932–2945.
27. Shankar SS, Rizzello L, Cingolani R, Rinaldi R, Pompa PP (2009) Micro/nano scale patterning of nanostructured metal substrates for plasmonic applications. *ACS Nano* 3:893–900.
28. Rizzello L, et al. (2009) Microscale patterning of hydrophobic/hydrophilic surfaces by spatially controlled galvanic displacement reactions. *Langmuir* 25:6019–6023.
29. Alberts A, et al. (2002) *Molecular Biology of the Cell* (Garland Science, New York).
30. Zaidel-Bar R, Itzkovitz S, Ma'ayan A, Iyengar R, Geiger B (2007) Functional atlas of the integrin adhesome. *Nat Cell Biol* 9:858–867.
31. Ziegler WH, Liddington RC, Critchley DR (2006) The structure and regulation of vinculin. *Trends Cell Biol* 16:453–460.
32. Humphries JD, et al. (2007) Vinculin controls focal adhesion formation by direct interactions with talin and actin. *J Cell Biol* 179:1043–1057.
33. Tanentzapf G, Martin-Bermudo MD, Hicks MS, Brown NH (2006) Multiple factors contribute to integrin-talin interactions in vivo. *J Cell Sci* 119:1632–1644.
34. Brocco MA, Panzetta P (1999) Survival and process regrowth of purified chick retinal ganglion cells cultured in a growth factor lacking medium at low density. Modulation by extracellular matrix proteins. *Dev Brain Res* 118:23–32.
35. Carri NG, Perris R, Johansson S, Ebendal T (1988) Differential outgrowth of retinal neurites on purified extracellular matrix molecules. *J Neurosci Res* 19:428–439.
36. Dumbauld DW, Michael KE, Hanks SK, Garcia AJ (2010) Focal adhesion kinase-dependent regulation of adhesive force involves vinculin recruitment to focal adhesions. *Biol Cell* 4:203–213.
37. McDonald PC, Fielding AB, Dedhar S (2008) Integrin-linked kinase—Essential roles in physiology and cancer biology. *J Cell Sci* 121:3121–3132.
38. Horton C, Ehlers MD (2003) Dual modes of endoplasmic reticulum-to-Golgi transport in dendrites revealed by live-cell imaging. *J Neurosci* 23:6188–6199.
39. Lu L, Tai G, Hong W (2004) Autoantigen Golgin-97, an effector of Arl1 GTPase, participates in traffic from the endosome to the trans-golgi network. *Mol Biol Cell* 15:4426–4443.
40. Nozawa K, et al. (2002) Fragmentation of Golgi complex and Golgi autoantigens during apoptosis and necrosis. *Arthritis Res* 4:R3 Available at http://arthritis-research.com/4/4/R3.